Instruments and Methods

Stability algorithm for snow micro-penetrometer measurements

Sascha BELLAIRE, Christine PIELMEIER, Martin SCHNEEBELI, Jürg SCHWEIZER

WSL Institute for Snow and Avalanche Research SLF, Flüelastrasse 11, CH-7260 Davos Dorf, Switzerland
E-mail: bellaire@slf.ch

ABSTRACT. Information on snow-cover stability is important for predicting avalanche danger. Traditionally, stability evaluation is based on manual observations of snow stratigraphy and stability tests, which are time-consuming. The SnowMicroPen (SMP) is a high-resolution, constant-speed penetrometer to measure penetration resistance. We have analysed the resistance signal to derive snow stability. The proposed stability algorithm was developed by comparing 68 SMP force–distance profiles with the corresponding manual profiles, including stability tests. The algorithm identifies a set of four potentially weak layers by taking into account changes in structure and rupture strength of microstructural elements that make up snow layers as derived from the SMP signal. In 90% of the cases, one of the four potentially weak layers proposed by the algorithm coincided with the failure layer observed in the stability test. To select the critical layer from the four potential weaknesses was more difficult. With fully automatic picking of the critical layer, agreement with the failure layer observed in the stability test was reached in 60% of the cases. To derive a stability classification, we analysed weak-layer as well as slab properties. These predictor variables allow the SMP signal to be classified into two stability classes, poor and fair-to-good, with an accuracy of ~75% when compared with observed stability. The SMP, in combination with the proposed algorithm, shows high potential for providing snow-cover stability information at high resolution in time and space.

INTRODUCTION

Prerequisites for the release of a dry-snow slab avalanche are a weak layer below one or more slab layers. The slab layers consist of cohesive, well-bonded snow with densities of ~200 kg m^{-3} and typical thicknesses of ~0.5 m (McClung and Schaerer, 2006). Dry-snow slab avalanches can be triggered by continuous loading during snowfall as well as by localized rapid near-surface loading by, for example, skiers. However, layers deeper than 1 m are rarely skier-triggered (Schweizer and others, 2003). Slab-avalanche release depends on weak-layer and slab properties, and their interaction. Habermann and others (2008) showed that hard layers impede failure initiation by skiers, but pointed out that they may favour fracture propagation. Weak layers underneath the slab typically consist of poorly bonded snow, such as depth hoar, surface hoar and faceted crystals. These grain types are formed under kinetic growth conditions and can reach grain sizes up to a few millimetres. Layers consisting of these large grains form fewer bonds per unit volume than layers of well-bonded grain types, such as small rounded grains. Due to their anisotropic structure, layers of poorly bonded grain types are weaker in shear than in compression (Akitaya, 1974, p. 39–40; McClung and Schaerer, 2006, p. 77).

Avalanche forecasting is based on information about the snow cover and its evolution in time. Snowpack-instability data are key elements in predicting avalanche danger. So far this information has been mainly derived from manual observations and stability tests. About 10 years ago, a high-resolution constant-speed penetrometer was developed to enable quick snowpack resistance probing (Schneebeli and Johnson, 1998). The method requires no digging and is comparable to the rammsonde, but unlike the rammsonde provides objective high-resolution data. It is possible to use the data to derive snow properties, based on a micro-mechanical model developed by Johnson and Schneebeli (1999). Previous studies analysed properties of specific weak layers, such as surface hoar layers, in space and time using various statistical methods (Birkeland and others, 2004; Kronholm and others, 2004; Lutz and others, 2007; Schweizer and Kronholm, 2007).

Pielmeier and others (2006) and Pielmeier and Schweizer (2007) related snow-layer properties derived from the SMP (SnowMicroPen, or snow micro-penometer) signal to snow-cover stability. They found that the failure-layer hardness and the differences in hardness between the failure layer and the adjacent layer, as well as the structural size, were indicators of instability. However, their approach requires foreknowledge of the location of the failure layer.

Satyawali and others (2009) related the mean, the standard deviation and the coefficient of variation of the SMP penetration resistance to the major grain types. With the help of some additional expert rules they suggested a method of relating SMP signal to grain types.

Floyer and Jamieson (2008) and Van Herwijnen and others (in press) used various signal-processing methods to identify known weak layers in penetrometer signals. Additionally, Floyer and Jamieson (2008) suggested a framework for the automatic detection of weak layers.

Weak-layer detection in manual observations seems similarly difficult. Schweizer and Jamieson (2007) related manually observed failure-layer properties to observed instability and developed a threshold-sum approach to classify failure layers, based on structural properties. When they used the method for failure-layer detection, i.e. identifying the principal weakness in a given snow stratigraphy, the accuracy was only 53%, exemplifying the difficulty of failure-layer detection.

Winkler and Schweizer (in press) compared different stability tests with regard to stability classification. They found that stability tests performed adjacent to each other revealed the same failure layer in only ~60% of cases and pointed out the challenge of automatically detecting potential failure layers within a snow cover.

Currently, no method exists which automatically identifies the most critical layer to be skier-triggered and estimates the corresponding degree of instability. We analysed 68 SMP profiles measured next to manual profiles and stability tests to develop a method that solves this problem step by step.

DATA

The proposed stability algorithm was developed with a dataset consisting of 68 SMP profiles from the eastern Swiss Alps that were measured close to (<0.5 m from) a manual snow profile completed with a stability test. Stability tests used were the rutschblock test (in 58 cases) (Föhn, 1987a) and the compression test (in 10 cases) (Jamieson, 1999).

In the following, the weak-layer properties and failure depth derived from the manually observed profiles are described. In ~49% of the 68 observed profiles the primary grain types in the failure layer were faceted crystals. In another 20 profiles, the failure layer primarily consisted of either depth hoar (16%), rounded facets (10%) or buried surface hoar (4%). In the remaining failure layers (21%) melt forms, graupel and mixtures of rounded grains and decomposed and fragmented precipitation particles were observed. The failure depth ranged from 5 to 58 cm, with a median value of 33 cm.

For the validation of the proposed SMP stability index, the profiles were grouped into two stability classes based on the rutschblock score. Scores ≤ 3 indicated 'poor' stability (N = 28), and scores ≥ 4 indicated 'fair-to-good' stability (N = 40). Compression test scores were converted into comparable rutschblock scores according to Schweizer and Jamieson (2003).

METHODS

Snow micro-penetrometer

The SMP consists of a probe which is driven by a motor with a constant speed of 20 mm s^{-1} into the snow cover (Schneebeli and Johnson, 1998). The movable cone-shaped tip, with a diameter of 5 mm and an included angle of 60°, transfers changes in penetration resistance to a piezoelectric sensor. The force sensor measures penetration resistance (range 0–42 N) every 4 µm, which corresponds to a data-sampling rate of 5 kHz. As most of the penetration resistance is due to the contact of the upper part of the cone (not the tip) with the ice matrix, it is assumed that the layer resolution of the SMP corresponds to the height of a truncated cone with a lateral area that is two-thirds of the lateral surface area of the whole cone, that is 1.8 mm. This resolution seems sufficient, as snow layers thinner than ~1 mm have not been observed in surface or thin sections (Matzl, 2006). A thickness of ~1 mm seems to be a lower bound caused by the sedimentation processes typical for snow.

Common practice while analysing SMP profiles in order to derive weak-layer properties is a visual inspection of the signal. Changes in penetration resistance are attributed to layer boundaries. A change in signal variance is also an indicator of changing snow types (Schneebeli and others, 1999). In combination with the manual profile and a stability test, experienced users can identify weak layers manually in the SMP profile. The boundaries of a snow layer in the SMP profile are not discrete, as suggested in manually observed profiles; instead a transition zone between two layers exists, i.e. the hardness changes gradually between two layers of different hardness. The transition zone is partly an artefact of the measuring device, since the measuring cone-shaped tip has a finite length (4.33 mm). Transition zones between layers with large differences in penetration resistance are of the order of the layer resolution, but can be larger within softer snow. These transition zones have to be taken into account when analysing the force–distance signal (Fig. 1).

Manual identification of weak layers is partly subjective, time-consuming and the weak layer has to be known. An automatic identification of the weak layer would substantially improve the applicability of the SMP.

Since the SMP is used under field conditions, the operator has to follow several procedures to ensure reliable SMP data acquisition. For instance, to avoid measurement errors due to variable SMP penetration speed, the operator has to hold the motor casing steady to prevent the device from lifting due to the reaction force of the SMP against the snow. Furthermore, the sensor is often subject to large temperature changes during the measurement. These temperature changes affect the casing surrounding the piezoelectric sensor, which results in a deformation of the piezo-crystal which may cause signal drift (Fig. 1). To minimize these effects, the SMP should be cooled before each measurement.

SMP microstructural model

Snow consists of sintered ice particles, and the strength of snow increases during the sintering process due to bond growth (Kaempfer and Schneebeli, 2007). The porosity of snow layers that are part of a dry-snow slab exceeds 70%. This high porosity allows the SMP to measure the deformation and failure of microstructural elements that can be used for a quantitative analysis of the SMP penetration profile.

To derive structural information, failures of individual microstructural elements need to be identified in the SMP signal. The SMP measures a force–distance profile. This force measurement in low-density snow (50–300 kg m^{-3}) is caused by the rupture and deflection of the microstructural elements, i.e. the rupture of bonds (Johnson and Schneebeli, 1999). In high-density snow (>300 kg m^{-3}), additionally, the friction between the ice and the sensor tip needs to be taken into account. A schematic SMP signal for two different snow types is shown in Figure 2. A microstructural element will rupture within a typical length of dimension L_n, and will induce a peak force in the SMP signal, F_{max} (Fig. 2c). The rupture force, f_r, is defined as the difference between the peak force, F_{max}, and the corresponding minima, F_{min}.

We used a signal-analysis routine described by Kronholm (2004), but with a negative threshold value, t_{fail} = –4.5 N mm^{-1}. We found this value to be more appropriate than the value originally used by Kronholm (2004) (t_{fail} = –2.0 N mm^{-1}), since a steeper threshold reduces the noise in the calculated rupture forces so that only relevant ruptures are detected. Furthermore, a different threshold value will only change the absolute values of different snow types and not the relative values relevant to this study.

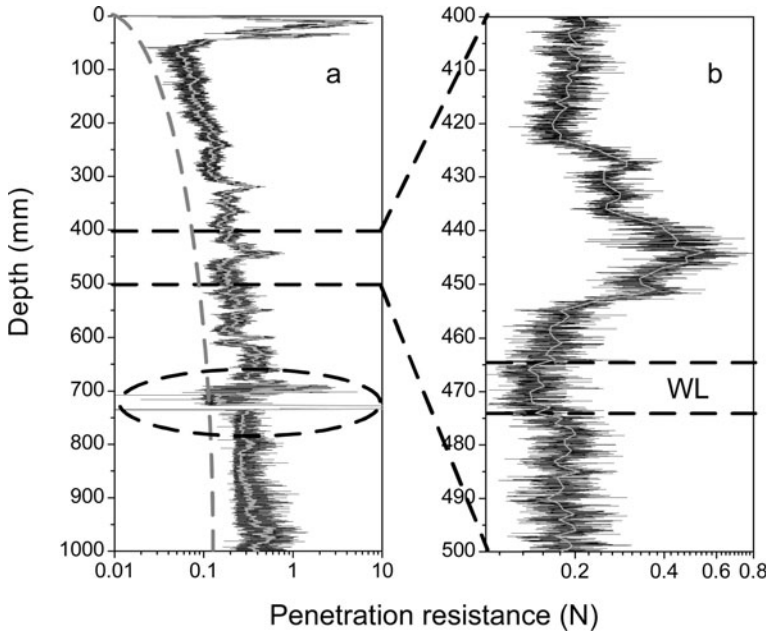

Fig. 1. (a) SMP signal on a logarithmic force scale (13 April 2005, eastern Swiss Alps). Dashed black lines indicate region of weak layer identified manually by visual inspection of the signal. Dashed grey curve shows the signal drift. Dashed circle indicates region of measurement errors (spikes) due to lifting of the SMP. Light grey solid line shows the average over 1 mm of signal. (b) Zoom to the region of the weak layer. Light grey solid curve shows the average over 1 mm of signal. Dashed black lines (465–475 mm) show manually chosen upper and lower boundaries of the weak layer.

SMP signal quality

The SMP signal can be affected by mechanical (frozen sensor) or electronic (temperature gradient) problems. The SMP signals used in this study were visually inspected to identify affected signals. Before the sensor tip touches the snow surface, the tip travels through the air while measuring. The signal measured in air should only be affected by vibrations from the motor and can be used as a baseline signal to identify erroneous signals. A typical air signal oscillates around zero with a maximum amplitude of ± 0.02 N, depending on the specific SMP. If the sensor is frozen, the amplitude is much smaller. Within the snow cover, an erroneous signal due to a frozen tip can be identified by a near-linear increase in penetration resistance. Erroneous SMP signals identified in this way were excluded from this study. Measurements which showed a negative or positive drift in the air signal were also excluded. This drift is typically due to electronic problems such as a damaged cable (stray capacitance), or when the sensor is affected by a large temperature gradient.

SMP signal interpretation

Johnson and Schneebeli (1999, fig. 4) compared SMP signals for different snow types and found that some snow types have unique SMP signals related to their microstructures. They showed that a wind slab has a ten times larger rupture force than snow consisting of depth hoar. The high rupture forces can be explained by the strongly sintered ice structure, i.e. a well-bonded structure. A weak layer can often be described as a region of poorly bonded grains, i.e. has few bonds per unit volume.

We interpret the SMP signal to distinguish between well-bonded and poorly bonded snow layers as a measure of snow slab instability. For a layer of well-bonded snow the rupture force, as well as the number of peaks, is expected to be large. Generally, a layer of poorly bonded snow can be identified by small rupture forces and a small number of peaks. However, in low-density snow the differences in rupture force and number of peaks between two types of snow are often not as distinct as in the examples described by Johnson and Schneebeli (1999). As small differences in the rupture force or the number of peaks between different layers may be crucial for weak-layer identification, the signal analysis is delicate, making the task of weak-layer detection challenging.

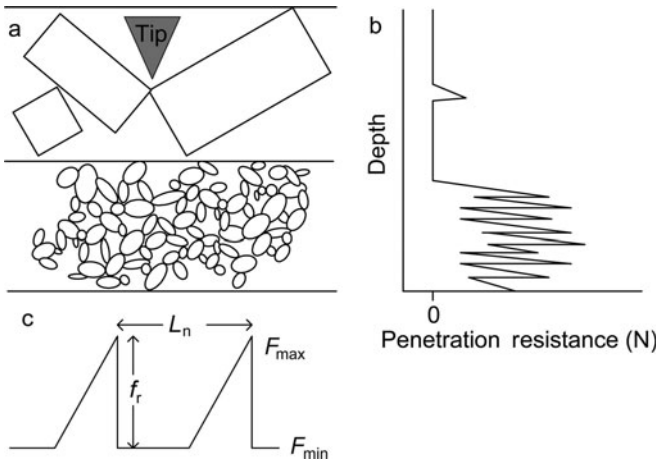

Fig. 2. (a) Schematic of poorly bonded (top) and well-bonded (bottom) snow layers and (b) the corresponding schematic SMP signals. (c) Definition of the microstructural parameters, rupture force, f_r, element length, L_n, and peak force, F_{max}, and the corresponding minimum, F_{min}. The number of peaks, n_{peaks}, corresponds to the number of ruptures per unit length.

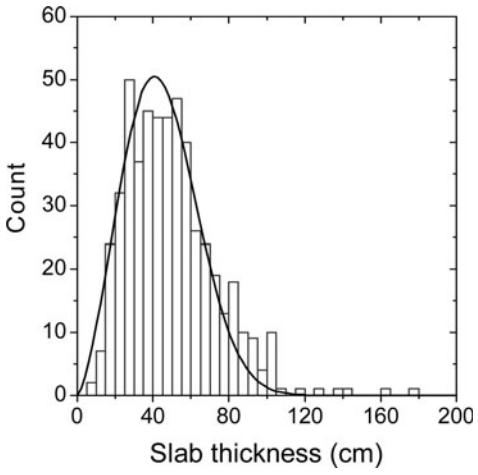

Fig. 3. Frequency distribution of slab thickness from 512 stability tests performed in the Swiss Alps and the Columbia Mountains of western Canada, and the fitted Weibull distribution (solid curve).

MODEL DEVELOPMENT AND TESTING

The proposed algorithm estimates stability by a stepwise sequential analysis of microstructural parameters derived from the SMP signal. First, the four weakest transitions between layers are identified. Second, for each of the four weakest transitions, the corresponding weak layer is defined. Third, by taking into account the layer structure, the weak layer that is most likely to fail is selected from the four potential weak layers. Finally, based on an analysis of weak-layer and slab properties, SMP signals are classified into two stability classes of ''poor' and 'fair-to-good'. This procedure is based on four assumptions:

1. The microstructural element length, L_n, is larger for poorly bonded snow than it is for well-bonded snow (Johnson and Schneebeli, 1999). As a consequence, the number of ruptures, n_{peaks}, per unit length is much smaller for poorly bonded snow than for well-bonded snow.
2. A weak layer can often be described as a region of poorly bonded grains, i.e. weaker bonds per unit volume. The rupture force, f_r, in a layer of poorly bonded grains is lower than the rupture force in a layer of well-bonded grains (Johnson and Schneebeli, 1999).
3. Large discontinuities in structure (hardness and grain size) between layers indicate weak areas or interfaces (Schweizer and Jamieson, 2003).
4. Weak layers buried deep within the snow cover are less prone to skier triggering, because the additional skier-induced stress strongly decreases with increasing depth (Föhn, 1987b; Schweizer and Camponovo, 2001).

As the first step, the SMP signal is averaged over 250 measurements, i.e. ~1 mm, and the parameters peak force, F_{max}, and rupture force, f_r, are averaged over each millimetre.

Detection of weak transitions

Following assumptions 1 and 2 above, a parameter, Ψ, is defined:

$$\Psi = \frac{\bar{f}_r \, n_{peaks}}{A}, \tag{1}$$

where $\bar{f}_r$ is the rupture force averaged over 1 mm of the SMP signal, n_{peaks} is the number of peaks over 1 mm and A is the lateral surface area of the sensor tip (~39 mm^2).

Parameter Ψ is smaller for poorly bonded than for well-bonded grain types (see assumptions 1 and 2 above). However, the minimum values of Ψ were not related to the observed locations of the weak layer. Furthermore, the location of the maximum element length is also often not related to the observed weak-layer location. This is partly because (a) soft snow, such as new snow, has a large element length and (b) slab layers that consist of soft snow often cannot be skier-triggered.

Following assumption 3, above, i.e. large discontinuities in properties between layers indicate a weakness, the gradient of Ψ is calculated over the whole signal. The gradient of Ψ, which can be interpreted as a boundary property, is only relevant for instability when the peak force is also small and indicates low strength. Therefore, the gradient of Ψ is scaled by the ratio of the peak force, F_{max}, to the lateral surface area, A, of the sensor tip:

$$B = \frac{A \nabla \Psi}{F_{max}}. \tag{2}$$

As F_{max} is typically smaller for poorly bonded layers than for well-bonded layers, sections of the SMP signal with $F_{max} >$ 0.5 N were not considered for further analysis.

In early winter, thick depth-hoar layers may form at the base of the snowpack. These may persist for the whole winter, but can usually not be triggered by skiers when they are buried deeper than ~1 m. However, in the SMP signal they are often identified as a weak transition, because Ψ is much smaller for larger grains than for smaller grains. To avoid this, parameter B was additionally weighted by a depth-dependent factor, w, derived from the frequency distribution of slab thickness. This factor corresponds to the Weibull density distribution:

$$w(z) = f(z, \alpha, \beta) = \frac{\alpha}{\beta} \; z^{\alpha-1} \, \mathrm{e}^{-\left(\frac{z}{\beta}\right)^{\alpha}}, \tag{3}$$

where z is the slab thickness, and α and β are the coefficients of the Weibull density distribution: α = 2.5, β = 500. This was fitted to the frequency distribution of thicknesses of snow slabs above the failure surface from 512 stability tests performed in Switzerland and Canada (updated from Schweizer and Jamieson, 2003) (Fig. 3). Without the weighting factor, w, the snow surface is, in most cases, identified as the weakest transition (air/snow).

Combining Equations (2) and (3) yields the final parameter, Δ, in seeking potential weaknesses in a SMP profile:

$$\Delta = \frac{A \nabla \Psi}{F_{max}} \; w(z). \tag{4}$$

Parameter Δ can be negative for transitions between poorly bonded layers and well-bonded layers, and positive for bonded/poorly bonded transitions, i.e. a potential weak transition (WT) is located where Δ reaches either a maximum or a minimum value (Fig. 4b). For further analysis, the two primary (minimum and maximum) and the two secondary extreme values, that were closer to the surface than the primary ones, were used. The analysis indicates (see below) that in most of the analysed profiles one of these four transitions was related to the observed failure depth found with a stability test. Transitions buried deeper than the two primary ones were not related to the observed failure depth derived from stability tests.

Definition of weak-layer boundaries

Parameter Δ identifies the four potential weak transitions, i.e. poorly bonded regions. Colbeck and others (1990) defined a layer as a stratum which is different in at least one respect (hardness, grain size, shape) from the strata above and below. To define the upper and lower boundaries of the potential weak layer, the minimum force, F_{WL}, within 1 cm above and below the weak transition (WT) is identified. If F_{WL} is found above the weak transition, WT is defined as the lower layer boundary, otherwise it is defined as the upper layer boundary. To define the other layer boundary the coefficient of variation (CV) is calculated. The local CV is defined as the standard deviation divided by the mean over 1 mm of penetration force signal. It is assumed that a layer boundary is located where the gradient of the CV is >0.1. The locations where this threshold is exceeded correspond to the upper and lower boundary, respectively. However, these upper and lower boundaries often fall within the transition zone. Therefore the final upper and lower boundaries are assumed to be located in the middle, between the boundaries and the position of the minimum force, F_{WL}. The value of 0.1 was derived empirically by comparing the gradient of the CV to the observed manual profiles and their layering.

Selection of critical weak layer

To decide which of the four potential weaknesses is most likely to be skier-triggered, parameter Ψ calculated with the rupture force and number of peaks averaged over the thickness of the weak layer divided by depth-dependent factor, $w(z)$, is used:

$$P = \frac{\Psi}{w(z)}. \quad (5)$$

Parameter P is smallest for poorly bonded layers at the depth where the Weibull distribution of slab thickness (Equation (3); Fig. 3) has its maximum, i.e. in the range 30–50 cm. The weak layer that shows the lowest value of P is selected as the critical weak layer.

Figure 4a–f summarizes the above procedure to identify the critical weak layer in a SMP signal for the example given in Figure 1. First, the SMP signal is averaged over 250 measurements, i.e. over 1 mm (Fig. 4a). Four extreme values of parameter Δ are identified (Fig. 4b). Transition 2 (Fig. 4b) was the observed weak layer in the rutschblock test (depth z_{WL} = 465 mm). Figure 4c–f shows the region of the weak layer for the penetration resistance, F, parameter Ψ, the rupture force, f_r, and the number of ruptures, n_{peaks}. Parameter Ψ (Fig. 4d) is equally small for persistent and non-persistent layers (Jamieson and Johnston, 1998), indicating similar bonded layers. The weak layer (transition 2) in this example is a layer of rounded facets below a layer of small rounded grains that is harder than the weak layer. The rupture forces (Fig. 4e) below and above the hard layer are quite similar. In fact, similar grain sizes were observed, supporting assumption 2, above. As a result, in this case, following Equation (1), Ψ can only be smaller if the number of ruptures is smaller, which is often the case for layers of poorly bonded grains (Fig. 4f). In the example shown, the layer of rounded facets has slightly fewer bonds than the layers above the harder layer. Figure 4 also shows the difficulty of detecting weak layers that have structural parameters similar to those of layers that are not weak. To determine which of the four potential weak layers is the most prone to skier triggering, the minimum value of Equation (5) is used. Including either slab properties, weak-layer properties or a combination of both did not improve the automatic picking of the critical weak layer.

Testing detection of the critical weak layer

In order to test the algorithm, we compared the depth of the automatically picked critical weak layer to the depth of the failure layer that was identified manually in the SMP profile with the help of the manual snow profile and the stability test.

As the manual weak-layer definition is subjective and the boundaries can often not be accurately defined, we assumed that the weak-layer boundaries identified by the algorithm matched the observation when the boundaries (top or bottom) fell within $\pm$1 cm of the observed location.

When applying the algorithm to the 68 SMP profiles using the above condition, in 90% of cases one of the four potentially weak layers derived from the SMP signal coincided with the observed weak layer (Fig. 5a).

Using Equation (5) to select one of the four potential weaknesses, the selected critical weak layer agreed with the observed weak layer in 60% of cases (Fig. 5b). When only the 61 profiles were considered where the observed weak layer coincided with one of the four weaknesses suggested by the algorithm, the accuracy increased to 67%.

For comparison, Figure 5c shows that the depth of the minimum penetration resistance (or strength) was poorly related to the observed failure depth. The agreement was only 10%. This implies that microstructural properties and micromechanical strength derived from the SMP signal are essential for weak-layer detection.

Stability estimation

To derive a stability classification, we contrasted the profiles from the two stability groups (poor, fair-to-good) for various weak-layer and slab properties (Fig. 6). Variables included the number of ruptures, the rupture force, parameter Ψ, the weak-layer penetration resistance, the mean penetration resistance of the slab and the maximum penetration resistance of the slab. For the comparison, only those 61 profiles were considered where one of the potential weaknesses was the observed weak layer. The weak layer was manually selected as described above.

The profiles rated poor had lower median values for all variables than the profiles rated fair-to-good. For all variables, except the weak-layer penetration resistance (p = 0.75), the observed differences were judged to be statistically significant ($p < 0.006$) based on a non-parametric Mann–Whitney U-test (Spiegel and Stephens, 1999). For the significant variables, a threshold value was determined using tree statistics (Breiman and others, 1998) that classifies the profiles into the two stability classes. The performance of the different classifiers is indicated with the unweighted average accuracy (RPC) (Wilks, 1995). Results are shown in Table 1. All classifiers show similar performance. For our dataset, the weak-layer parameter, Ψ, discriminated best (RPC = 78%) between poor and fair-to-good profiles.

DISCUSSION

The proposed algorithm detects structural weaknesses in a SMP signal. Whereas in most cases one of the four potential weaknesses derived from the SMP signal coincided with the observed weak layer (manual selection), the fully automatic

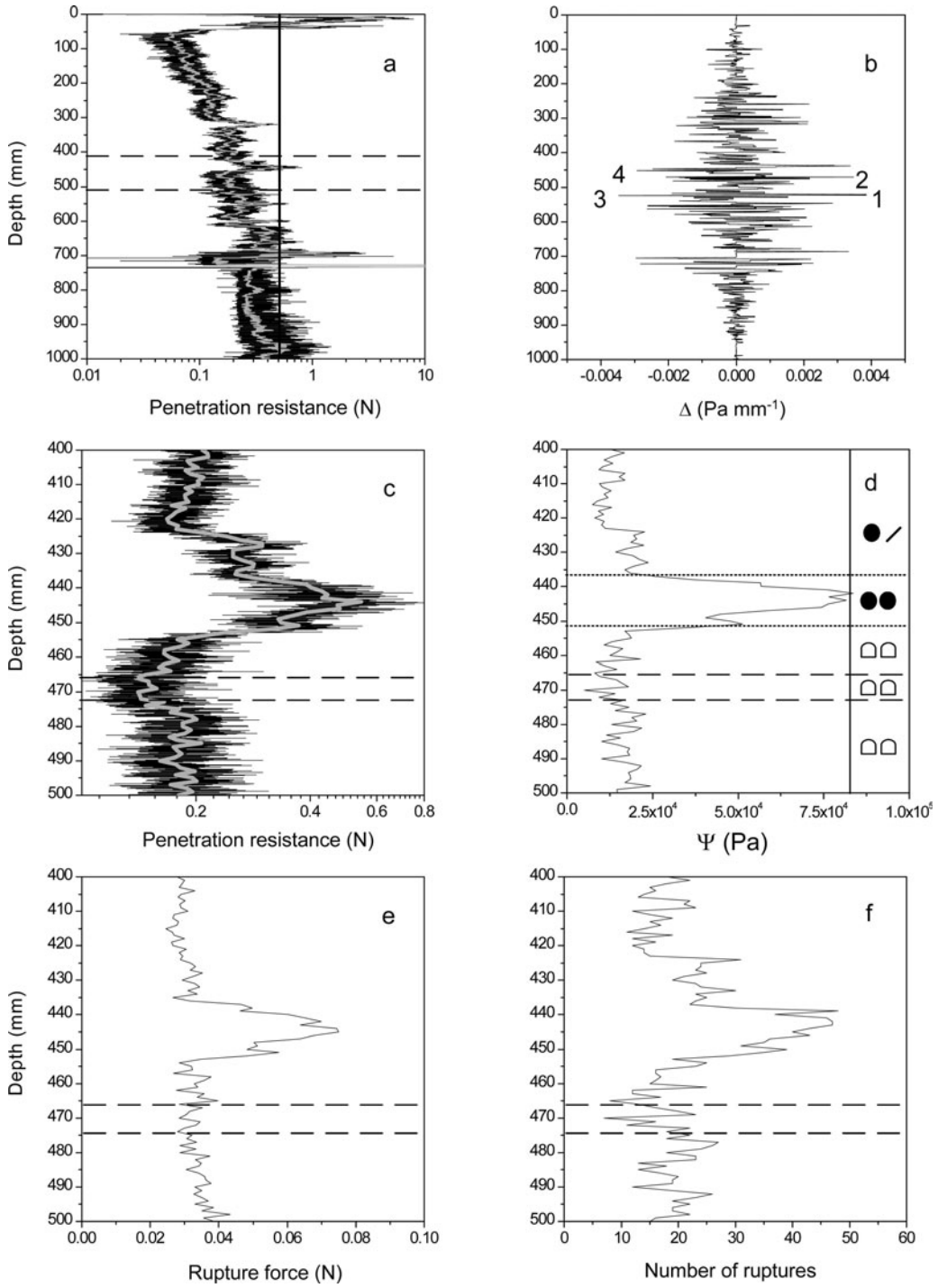

Fig. 4. (a) Original (black solid) and averaged SMP signal (grey solid line, 1 mm average). (b) Parameter Δ to find potential weak transitions. The locations are indicated by numbers 1–4. (c) Zoom to the region of weak layer (dashed lines in (a)) with original (solid black curve) and averaged (solid grey curve) SMP signal. Dashed lines show upper and lower boundaries indicated by the algorithm. (d) Parameter Ψ at the depth of the weak layer, with schematics indicating grain types for both the observed weak layer and adjacent layer. (e) Averaged rupture force for the depth of the weak layer. Dashed lines show layer boundaries of the weak layer. (f) Number of ruptures for the region of the weak layer. Dashed lines show upper and lower boundaries of the weak layer defined by the algorithm.

weak-layer detection by subsequently applying Equation (5) did not provide satisfactory results. However, the obtained accuracy is comparable to the performance of stability field tests such as the compression test or extended column test (Winkler and Schweizer, in press). These stability tests performed adjacent to each other identified the same weak layer only in ~60% of cases.

Some of the lack of accuracy might be due to technical problems with the SMP. The sensitivity of the SMP sensor to temperature changes might have caused erroneous signals that affected the layer boundary definition. This signal drift, i.e. positive or negative offset, can often not be recognized by a visual inspection and might affect the derivation of the structural properties.

Weak-layer as well as slab properties were tested to classify the measured SMP profiles into stability classes of poor and fair-to-good (Table 1). All variables provided plausible results. Poor stability is expected with a low number of

ruptures, low rupture force and a low value of Ψ in the weak layer, and with rather soft slab layers. The latter finding agrees with results of Habermann and others (2008) who found that hard layers within the slab impede failure initiation. A larger dataset would certainly improve the stability estimation and might also allow a multivariate approach.

Weak-layer detection and stability estimation is based on a single SMP measurement which is compared to a manual profile and a stability test that cannot be done at exactly the same location. Some spatial variations in layer properties may occur between the location of the SMP measurement and the location of the rutschblock. The uncertainty in the stability test result ($\pm$1 score) may further affect the results of the stability classification since only two stability classes were used.

A set of SMP measurements, covering the area of the rutschblock up to the slope scale, would improve the reliability of weak-layer detection. Furthermore, this would allow spatially related layer properties that favour fracture propagation to be determined, and taken into account for automatic weak-layer detection and stability estimation.

Nonetheless, the SMP, in combination with the algorithm and standard field observations (rutschblock test plus manual profile), can be used to quantify and analyse spatial-variability patterns faster than using standard observation methods.

CONCLUSIONS

We have developed an algorithm for the analysis of SMP profiles that detects a potential weakness and provides a stability estimate, and tested the procedure with 68 manually observed profiles. The algorithm suggests a set of four potential weak layers, and, in 90% of the cases, one of these weak layers coincided with the observed failure layer in the stability test. A fully automatic detection of the layer most prone to skier triggering identified the weak layer as observed with an accuracy of 60% and needs to be improved. A statistical analysis of weak-layer and slab properties was carried out for a subset of 61 profiles, in order to classify the SMP signals into two stability classes: poor and fair-to-good. With an accuracy of 78%, parameter Ψ was the best predictor of snowpack instability with regard to skier triggering.

The proposed algorithm, which is essentially a statistical method, is the first successful attempt to locate potential weak layers in a SMP signal and to suggest a degree of instability with regard to skier triggering. Obviously, the automatic detection of the weak layer that is most prone to be

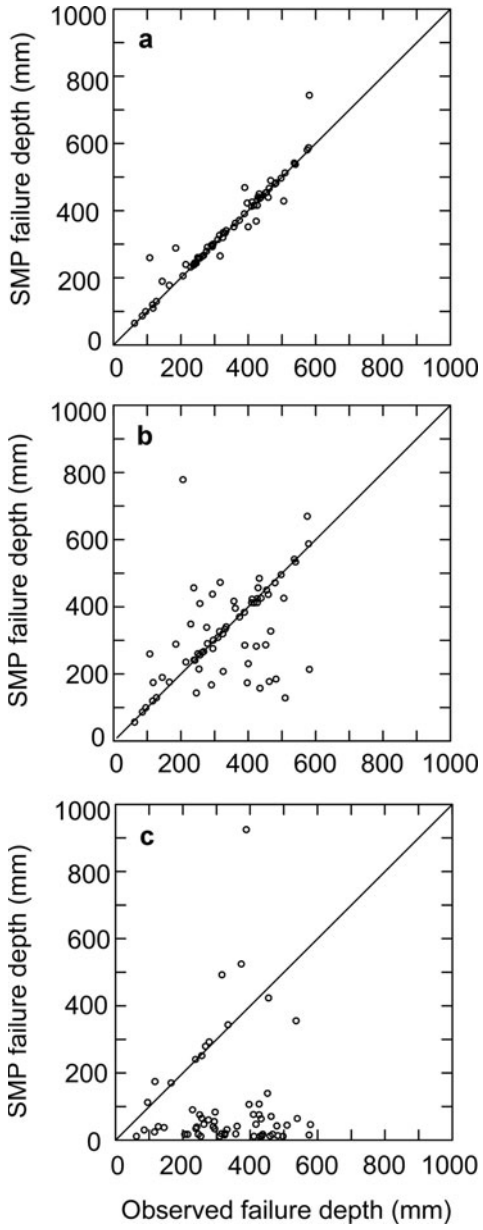

Fig. 5. (a) Failure depth derived from rutschblock test and compression tests vs failure depth selected manually from the four suggested weak layers (accuracy 90%). (b) Comparison of the observed failure depth to the failure depth of the weak layer derived with Equation (5) (accuracy 60%). (c) Comparison of the position of the lowest measured penetration resistance to the observed failure depth (accuracy 10%). The solid line in each graph shows the one-to-one relationship.

Table 1. Threshold values, classification accuracy and level of significance, p (U-test), for various weak-layer and slab properties. Values smaller than the threshold indicate poor stability. The classification accuracy is given by the unweighted average accuracy (RPC)

Parameter	Threshold	RPC	p
		%	
Mean number of ruptures per 1 mm	<7	75.7	<0.001
Mean rupture force (N) per 1 mm	<0.03	73.0	<0.001
Ψ of weak layer (Pa)	<5193	78.4	<0.001
Mean penetration resistance of slab (N)	<0.21	77.5	0.006
Mean penetration resistance of weak layer (N)	—	—	0.75
Maximum penetration resistance of slab (N)	<0.65	72.4	0.002

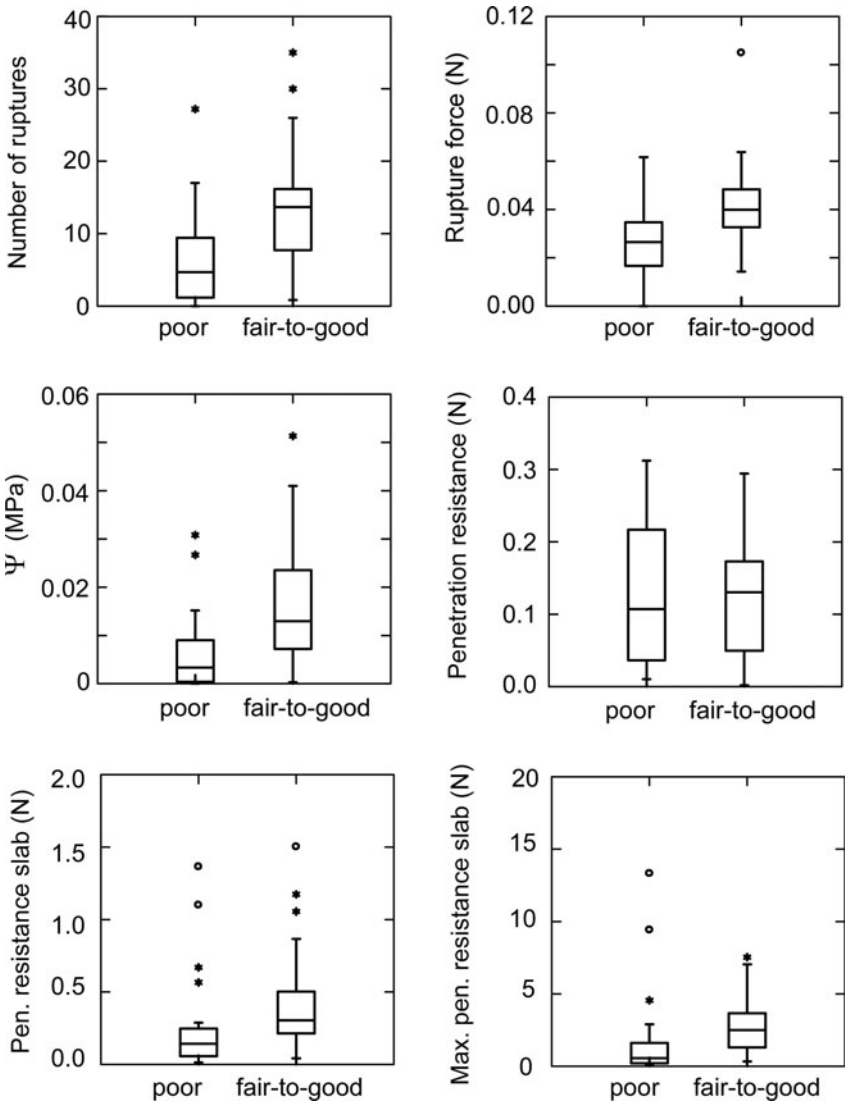

Fig. 6. Box plots of weak-layer and slab properties for the two stability classes observed (N = 61). Variables are the number of ruptures, the rupture force, parameter Ψ, the weak-layer penetration resistance, the mean penetration resistance of the slab and the maximum penetration resistance of the slab. Boxes span the interquartile range from first to third quartile, with the horizontal line showing the median. Whiskers show the range of observed values that fall within 1.5 times the interquartile range above and below the interquartile range.

skier-triggered needs to be improved. However, it has been previously shown that detecting weak layers is, in general, a very difficult problem and field tests do not perform any better. Furthermore, our results suggest that the presently used microstructural parameters are not sufficient for describing the complex interaction between the SMP tip and the ice matrix. In summary, the partly insufficient performance can be attributed to the limitations of the algorithm, poor SMP signal quality, spatial variations at the scale of the profile site and uncertainty of the stability test result.

Our analysis confirms that snowpack stability is not simply a question of minimal strength, but a complex interaction between weak-layer and slab properties (e.g. Schweizer and Jamieson, 2001). The somewhat unsatisfactory result is probably not only caused by our method of analysis, but also by the fact that snowpack instability cannot be measured objectively and by our general lack of understanding of the failure processes leading to avalanche release.

The SMP together with the proposed algorithm shows high potential for snow-cover investigations that require high-resolution data in time and space, which is needed for research on stability variations, as well as for operational avalanche forecasting.

ACKNOWLEDGEMENTS

This study was part of the TRIGS (triggering of instabilities in materials and geosystems) project funded by the European Commission (FP6-NEST). Comments by the scientific editor, S. Jones, and by J.B. Johnson and an anonymous reviewer helped to significantly improve the paper and were much appreciated.

REFERENCES

Akitaya, E. 1974. Studies on depth hoar. *Contrib. Inst. Low Temp. Sci., Ser. A,* 26,

Birkeland, K., K. Kronholm, M. Schneebeli and C. Pielmeier. 2004. Changes in the shear strength and micro-penetration hardness of a buried surface-hoar layer. *Ann. Glaciol.,* **38**, 223–228.

Breiman, L., J. Friedman, C.J. Stone and R.A. Olshen. 1998. *Classification and regression trees.* Boca Raton, FL, CRC Press.

Colbeck, S.C. *and 7 others*. 1990. The international classification for seasonal snow on the ground. Wallingford, Oxon, International Association of Hydrological Sciences. International Commission on Snow and Ice.

Floyer, J. and J.B. Jamieson. 2008. Avalanche weak layer tracing and detection in snow penetrometer profiles. *In* Locat, J., D. Perret, D. Turmel, D. Demers and S. Leroueil, *eds. Proceedings of the 4th Canadian Conference on Geohazards: From Causes to Management, 19–24 May 2008, Québec City, Que*. Québec, Presse de l'Université Laval, 161–168.

Föhn, P.M.B. 1987a. The 'rutschblock' as a practical tool for slope stability evaluation. *IAHS Publ.* 162 (Symposium at Davos 1986 – *Avalanche Formation, Movement and Effects*), 223–228.

Föhn, P.M.B. 1987b. The stability index and various triggering mechanisms. *IAHS Publ.* 162 (Symposium at Davos 1986 – *Avalanche Formation, Movement and Effects*), 195–214.

Habermann, M., J. Schweizer and J.B. Jamieson. 2008. Influence of snowpack layering on human-triggered snow slab avalanche release. *Cold Reg. Sci. Technol.,* **54**(3), 176–182.

Jamieson, J.B. 1999. The compression test – after 25 years. *Avalanche Rev.,* **18**(1), 10–12.

Jamieson, J.B. and C.D. Johnston. 1998. Refinements to the stability index for skier-triggered dry-slab avalanches. *Ann. Glaciol.,* **26**, 296–302.

Johnson, J.B. and M. Schneebeli. 1999. Characterizing the microstructural and micromechanical properties of snow. *Cold Reg. Sci. Technol.,* **30**(1–3), 91–100.

Kaempfer, T.U. and M. Schneebeli. 2007. Observation of isothermal metamorphism of new snow and interpretation as a sintering process. *J. Geophys. Res.,* **112**(D24), D24101. (10.1029/2007JD009047.)

Kronholm, K. 2004. Spatial variability of snow mechanical properties with regard to avalanche formation. (PhD thesis, University of Zürich.)

Kronholm, K., M. Schneebeli and J. Schweizer. 2004. Spatial variability of micropenetration resistance in snow layers on a small slope. *Ann. Glaciol.,* **38**, 202–208.

Lutz, E., K.W. Birkeland, K. Kronholm, K. Hansen and R. Aspinall. 2007. Surface hoar characteristics derived from a snow micropenetrometer using moving window statistical operations. *Cold Reg. Sci. Technol.,* **47**(1–2), 118–133.

Matzl, M. 2006. Quantifying the stratigraphy of snow profiles. (PhD thesis, ETH Zürich.)

McClung, D. and P. Schaerer. 2006. *The avalanche handbook. Third edition.* Seattle, WA, The Mountaineers.

Pielmeier, C. and J. Schweizer. 2007. Snowpack stability information derived from the SnowMicroPen signal. *Cold Reg. Sci. Technol.,* **47**(1–2), 102–107.

Pielmeier, C., J. Schweizer and H.P. Marshall. 2006. Improvements in the application of the SnowMicroPen to derive stability information for avalanche forecasting. *In* Gleason, J.A., *ed. Proceedings of the International Snow Science Workshop, 1–6 October 2006, Telluride CO, October 1–6, 2006*. 187–192. CD-ROM.

Satyawali, P.K., M. Schneebeli, C. Pielmeier, T. Stucki and A.K. Singh. 2009. Preliminary characterization of Alpine snow using SnowMicroPen. *Cold Reg. Sci. Technol.,* **55**(3), 311–320.

Schneebeli, M. and J.B. Johnson. 1998. A constant-speed penetrometer for high-resolution snow stratigraphy. *Ann. Glaciol.,* **26**, 107–111.

Schneebeli, M., C. Pielmeier and J.B. Johnson. 1999. Measuring snow microstructure and hardness using a high resolution penetrometer. *Cold Reg. Sci. Technol.,* **30**(1–3), 101–114.

Schweizer, J. and C. Camponovo. 2001. The skier's zone of influence in triggering slab avalanches. *Ann. Glaciol.,* **32**, 314–320.

Schweizer, J. and J.B. Jamieson. 2001. Snow cover properties for skier triggering of avalanches. *Cold Reg. Sci. Technol.,* **33**(2–3), 207–221.

Schweizer, J. and J.B. Jamieson. 2003. Snowpack properties for snow profile analysis. *Cold Reg. Sci. Technol.,* **37**(3), 233–241.

Schweizer, J. and J.B. Jamieson. 2007. A threshold sum approach to stability evaluation of manual snow profiles. *Cold Reg. Sci. Technol.,* **47**(1–2), 50–59.

Schweizer, J. and K. Kronholm. 2007. Snow cover spatial variability at multiple scales: characteristics of a layer of buried surface hoar. *Cold Reg. Sci. Technol.,* **47**(3), 207–223.

Schweizer, J., J.B. Jamieson and M. Schneebeli. 2003. Snow avalanche formation. *Rev. Geophys.,* **41**(4), 1016. (10.1029/2002RG000123.)

Spiegel, M.R. and L.J. Stephens. 1999. *Schaum's outline of theory and problems of statistics. Second edition.* New York, McGraw-Hill.

Van Herwijnen, A., S. Bellaire and J. Schweizer. In press. Comparison of micro structural snowpack parameters compressions tests. *Cold Reg. Sci. Technol.*

Wilks, D.S. 1995. *Statistical methods in the atmospheric sciences.* San Diego, CA, Academic Press.

Winkler, K. and J. Schweizer. In press. Comparison of snow stability tests: extended column test, rutschblock test and compression test. *Cold Reg. Sci. Technol.*

MS received 8 August 2008 and accepted in revised form 7 May 2009